

Synthesis, Structural Characterization and Solid-State NMR Studies of New Defect Pyrochlore-Type Antimoniates $(\text{H}_3\text{O}^+)_{0.36}\text{Ln}_x\text{Sb}_2\text{O}_{6+Y}$ (with $\text{Ln}=\text{Gd}^{3+}$, Eu^{3+} and $0 < X, Y < 1$) Prepared by Exchange Method

El Haimouti A^{1*}, Dubois M², Zambon D², El Ouafi T¹, El Mohammed MA¹ and Daoud M³

¹Laboratory of Chemistry and Mathematical Modelling, Department of Physics, Khouribga, University of Hassan, Morocco

²Laboratory of Inorganic Materials, UMR CNRS 6002, Blaise Pascal University, Aubière Cedex, France

³Mineral Solid Chemistry Laboratory, Department of Chemistry, Marrakech, Morocco

*Corresponding author: El Haimouti A, Laboratory of Chemistry and Mathematical Modelling, Department of Physics, Faculty Polydisciplinaire, Khouribga, University of Hassan, Morocco, Tel: +212-667 130655; E-mail: elhaimouti@yahoo.fr

Received: December 20, 2017; Accepted: January 12, 2017; Published: January 16, 2018

Abstract

A new cubic nonstoichiometric pyrochlore type antimoniates $(\text{H}_3\text{O}^+)_{0.36}\text{Ln}_x\text{Sb}_2\text{O}_{6+y}$ (with $\text{Ln} = \text{Gd}^{3+}$, Eu^{3+} and $0 < x, y < 1$) have been prepared by exchange method starting from $\text{Na}_{0.36}\text{Gd}_{0.80}\text{Sb}_2\text{O}_{6.38}$ compound. Their crystal structures were investigated by Rietveld refinement and further confirmed both by infrared spectroscopy and by MAS-NMR experiments. In these defect pyrochlores the 16d positions of space group F d_{3m} ($n^\circ 127$) is occupied by rare earth ions, the 48f positions by O^{2-} and the 8b positions by O^{2-} and H_3O^+ .

Keywords: Pyrochlore; Exchange method; X-Ray diffraction; Infrared spectra; Magic angle spinning; Nuclear magnetic resonance

Introduction

The study of the solid protonic conductors constitutes a field of investigation in the range of the physiochemistry of materials. Many researchers showed the potential of the oxides pyrochlores such as NH_4TaWO_6 [1], MNbWO_6 ($\text{M}=\text{H}$ [2] or NH_4 [3]), $\text{Na}^+(\text{NaTaWO}_6$ [4], $\text{K}^+(\text{K}_{1+x}\text{W}_{1-x}\text{O}_6$ [5]), $\text{Rb}^+(\text{Rb}_{3/2}\text{Cr}_{1/2}\text{Te}_{3/2}\text{O}_6$ [6] and $\text{Ti}^+(\text{Ti}_{1+x}\text{Ta}_{1-x}\text{W}_{1-x}\text{O}_6$ [7]) for ionic conduction. Duan et al showed that the exchange properties of the hydroxylated phases $\text{KTa}_2(\text{O}, \text{OH})_6$ exhibit interesting catalytic properties [8]. Moreover, the hygroscopicity of some of these compounds can be considered an asset. Since the conductivity of pyrochlores with formula $(\text{M}_2\text{O})_x\text{WO}_3 \cdot z\text{H}_2\text{O}$ ($\text{M}=\text{H}^+$, Li^+ , Na^+ , Ag^+ , NH_4^+) is strongly dependent of the degree of hygroscopy of the medium, these compounds can then be used as sensors of moisture [9]. In fact, intense research during these last years is devoted to the development of new ion exchanger materials.

Citation: El Haimouti A, Dubois M, Zambon D, et al. Synthesis, Structural Characterization and Solid-State NMR Studies of New Defect Pyrochlore-Type Antimoniates $(\text{H}_3\text{O}^+)_{0.36}\text{Ln}_x\text{Sb}_2\text{O}_{6+Y}$ (with $\text{Ln}=\text{Gd}^{3+}$, Eu^{3+} and $0 < X, Y < 1$) Prepared by Exchange Method. Int J Chem Sci. 2018;16(1):238

© 2018 Trade Science Inc.

In addition to many works concerned the exchange properties of lamellar perovskite type containing niobate [10-12], some antimonates were also investigated [13-15]. One of approach of the problem, already tested successfully for various ions, consists to take into account the structural aspect: the structure is characterized by an open framework, favouring the ionic mobility. Accordingly, synchexs protonic conductor performed, for example, by substitution of a monovalent ion, generally alkaline ion.

Some protonic conductors can be directly prepared; as exemplified by HUP ($\text{HUO}_2\text{PO}_4, 4\text{H}_2\text{O}$) which results from the reaction of the phosphoric acid on uranyl nitrate [16]. An indirect preparation is also possible: it consists in substituting by acid way a monovalent element in structural materials likely to allow a good ionic mobility. This approach leads to the synthesis of the phases $\text{HMO}_3, x\text{H}_2\text{O}$ or $\text{M}=\text{Sb, Nb and Ta}$ [17], pyrochlores $\text{HNbWO}_6 \cdot x\text{H}_2\text{O}$ [18] and NH_4NbWO_6 [19].

Recently, we reported the conditions to obtain new defect pyrochlores in the systems ($\text{A}=\text{Na, K, Rb, Cs or Tl}$; $\text{Ln}=\text{Y, Gd and Eu}$)- Sb-O [20,21]. Because their high content of defects, ionic exchange properties could be expected for these pyrochlores. It appeared interesting to investigate the exchange in aqueous medium of the sodium ion by a monovalent ion such as hydronium H_3O^+ and ammonium NH_4^+ ions in the $\text{Na}_{0,36}\text{Ln}_x\text{Sb}_2\text{O}_{6+y}$ phase. This process could be facilitated for three main factors:

- Position of the Na^+ cations in large-sized cages, suggesting a high mobility of the charge carriers.
- Presence of the defect in the sites occupied by sodium.
- Insolubility of the materials.

The ideal structure of pyrochlore $\text{A}_2\text{B}_2\text{X}_6\text{X}'$ (or $\text{AA}'\text{B}_2\text{X}_6\text{X}'$) has been previously described [22-25]. The crystal structure exhibits a three-dimensional framework builds with edge-sharing regular BX_6 octahedra and sharing channels along the $\langle 110 \rangle$ directions. The cages, centred on the positions 8b (3/8, 3/8, 3/8) and occupied by the X' ion, are created by the intersection of six channels. Because of their large size, they can theoretically accommodate ions with ionic radius less than or equal to 1.80 Å, approximately and surrounded by 18 anions X.

The synthesis and the structural characterization of new pyrochlores with composition $(\text{H}_3\text{O}^+)_{0,36}\text{Ln}_x\text{Sb}_2\text{O}_{6+y}$ (with $\text{Ln}=\text{Gd}^{3+}, \text{Eu}^{3+}$ and $0 < x, y < 1$) obtained by exchange method have been investigated in this this work. Infrared spectroscopy and ^{23}Na and ^1H MAS-NMR measurements were performed in order to confirm the ionic exchange.

Experimental

The $(\text{H}_3\text{O}^+)_{0,36}\text{Gd}_{0,80}\text{Sb}_2\text{O}_{6,38}$ and $(\text{H}_3\text{O}^+)_{0,36}\text{Eu}_{0,82}\text{Sb}_2\text{O}_{6,41}$ compounds were prepared by exchange method. FIG. 1 displays the experimental process used for the synthesis of the samples. The starting materials for the preparation of $\text{Na}_{0,36}\text{Ln}_x\text{Sb}_2\text{O}_{6+y}$ was $\text{NaNO}_3, \text{Sb}_2\text{O}_3$ and $\text{Ln}_2\text{O}_3, 6\text{H}_2\text{O}$. The preparation for this compound was carried out by using the same method as previously described [20].

The $\text{Na}_{0,36}\text{Ln}_x\text{Sb}_2\text{O}_{6+y}$ agitated by magnetic stirring for 48 hours and then treated by a hydrochloric solution (0.1 M). The obtained powders are separated from the solution by filtration and were oven-dried at 100°C for 12 hours. The X-ray analysis reveals that pure pyrochlore phases were obtained and the characterization of the filtrate obtained after exchange shows the formation of sodium chloride what is in favour of the exchange.

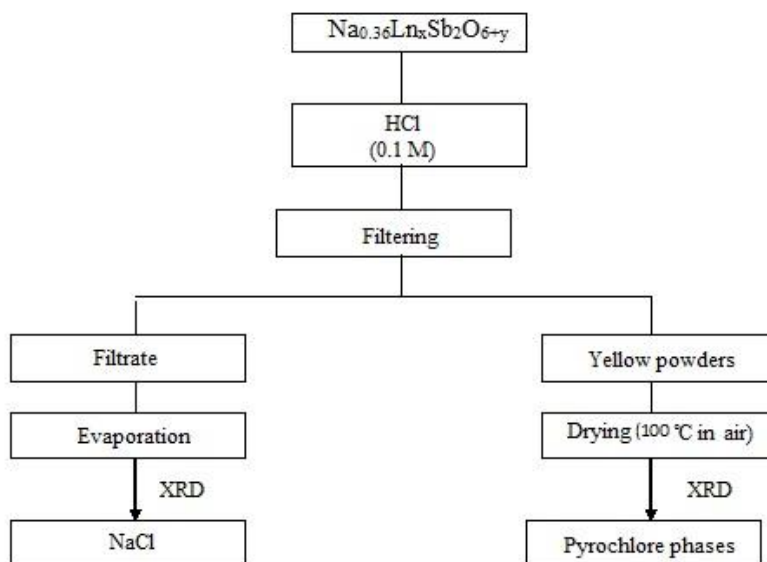


FIG. 1. Experimental procedure for the synthesis of $(\text{H}_3\text{O}^+)_{0.36}\text{Ln}_x\text{Sb}_2\text{O}_{6+y}$ compounds (with $\text{Ln}=\text{Gd}, \text{Eu}$ and $0 < x, y < 1$).

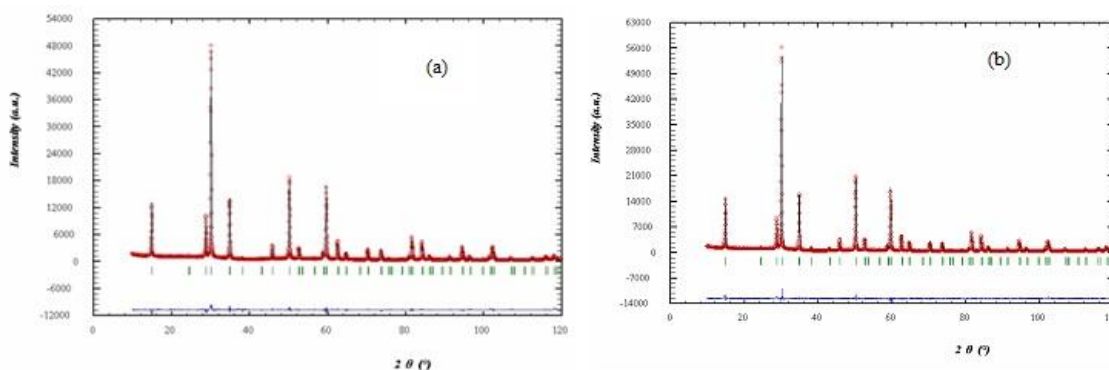


FIG. 2. Observed, calculated and difference X-ray powder diffraction patterns for $(\text{H}_3\text{O}^+)_{0.36}\text{Gd}_{0.80}\text{Sb}_2\text{O}_{6.38}$ (a) $(\text{H}_3\text{O}^+)_{0.36}\text{Eu}_{0.82}\text{Sb}_2\text{O}_{6.41}$ (b) The observed data are represented by dots and the calculated ones by the solid line.

The structural characterization of the resulting powders by the Rietveld method [26] was performed from X-ray powder patterns recorded on the 2θ range 10° to 120° with a step scan of 0.028° using a SIEMENS D-501 diffractometer (λ of $\text{CuK}\alpha=1.5405 \text{ \AA}$). The data processing was performed using the FULLPROF program [27].

Fourier-transform infrared spectroscopy performed with a spectrophotometer with Fourier transform NICOLET 55XC. The sample spectra were recorded by transmission in a dry air atmosphere between 400 cm^{-1} and 4000 cm^{-1} . X spectra accumulation was performed through a pellet made of 2 mg of the sample material deluted in KBr (200 mg).

The ^1H and ^{23}Na NMR spectra were recorded at room temperature with a Bruker MSL300 spectrometer operating at 300.1 and 79.4 MHz respectively for ^1H and ^{23}Na experiments. MAS spectra were performed at 8 KHz with Bruker 4 mm MAS probes using a simple sequence (τ - acquisition). The processing and acquisition parameters were recycling at time 0.5 and 6 s, 5 and 6 μs single $\pi/2$ pulse duration and 64 and 2400 scans for ^1H and ^{23}Na NMR measurements, respectively. The ^1H chemical shifts are given in ppm and referred to tetramethylsilane (TMS) by using adamantane as an external standard (1.74

ppm from TMS). The chemical shifts for ^{23}Na NMR experiments are quoted relative to NaCl (solid) as external standard referenced to 0 ppm. The reproducibility of the measured chemical shift values was in order to 0.1 ppm.

Results and Discussion

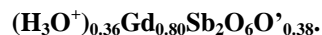
Crystallographic study

The obtained $(\text{H}_3\text{O}^+)_{0.36}\text{Gd}_{0.80}\text{Sb}_2\text{O}_{6.38}$ and $(\text{H}_3\text{O}^+)_{0.36}\text{Eu}_{0.82}\text{Sb}_2\text{O}_{6.41}$ compounds exhibit a yellow colour. The X-ray powder patterns of these compounds were indexed in the cubic system with the space group F d3m ($n^\circ 127$). The element of framework (Sb_2O_6) were positioned on the sites 16 (c) (0, 0, 0) and 48 (f) (x, 1/2, 1/2) respectively for antimony and oxygen atoms as for pyrochlores $\text{Na}_{0.36}\text{Ln}_x\text{Sb}_2\text{O}_{6+y}$ [20]. The scattering factors were used supposing that the elements are in an ionic state, those of H_3O^+ ions are identical to atomic oxygen having the same number of electrons.

XRD powder study does not allow to precisely locating the hydronium ions taking into account scattering factor of oxygen atom in comparison with the metal elements. By analogy with the pyrochlore $\text{Na}_{0.36}\text{Ln}_x\text{Sb}_2\text{O}_{6+y}$ [20], both H_3O^+ and Ln cations are located on 16 (d) sites (1/2,1/2,1/2). The reliability factors obtained during the refinement are unsatisfactory ($R_B > 16$); nevertheless, this permits to exclude the hypothesis of the occupation of the 16 (d) sites by the hydronium ions.

In order to obtain better reliability factors, one second assumption was done consisting of a statistical occupation of the 8 (b) sites (3/8,3/8,3/8) by the hydronium and oxygen (O') ions; isotropic thermal displacement parameters for these ions were selected by analogy with pyrochlore $\text{K}_{0.42}\text{Eu}_{0.74}\text{Sb}_2\text{O}_{6.32}$ [20]. After refinement, the reliability factors R_B converge towards satisfactory values (TABLE 1) confirming the statistical and alternative occupation of the site 8 (b) by either H_3O^+ or O' ions and a partial occupation of the 16d sites by rare earth ions with site occupancy factors less than 0.5. When H_3O^+ (resp. O') occupies the 8 (b) sites, the 16 (d) position is vacant (resp. occupied). The atomic coordinates the isotropic thermal displacement parameters, the occupancy factors, the reliability factors and the unit cell parameters are gathered in TABLE 1. The mean interatomic distances and bond angles are listed in TABLE 2. The observed cations-oxygen bond distances are in good agreement with sum of the ionic radii [28] and compatible with a statistical repartition of H_3O^+ and O' ions over the 8 (b) sites. The observed, calculated and difference patterns for $(\text{H}_3\text{O}^+)_{0.36}\text{Ln}_x\text{Sb}_2\text{O}_{6+y}$ are shown in FIG. 2.

TABLE 1. Atomic coordinates, isotropic thermal parameters B (\AA^2), relative occupancies τ , reliability factors and unit cell parameters in $(\text{H}_3\text{O}^+)_{0.36}\text{Ln}_x\text{Sb}_2\text{O}_6\text{O}'_y$



Atoms	Wyckoff	x/a	y/b position	z/c	B (\AA^2)	τ
Gd	16 (d)	1/2	1/2	1/2	3.13 (4)	0.39
Sb	16 (c)	0	0	0	1.50 (3)	1
O	48 (f)	0.3294 (2)	0.125	0.125	4.83 (9)	1
H_3O^+	8 (b)	0.375	0.375	0.375	1.48 (5)	0.36
O'	8 (b)	0.375	0.375	0.375	1.48 (5)	0.36
-	$R_p = 10.90$	$R_{wp} = 10.90$	$\chi^2 = 4.26$	$R_B = 4.31$	$R_F = 4.28$	$a = 10.2829$ (7) \AA
$(\text{H}_3\text{O}^+)_{0.36}\text{Eu}_{0.82}\text{Sb}_2\text{O}_6\text{O}'_{0.41}$						
Atoms	Wyckoff	x/a	y/b	z/c	B (\AA^2)	τ position
Eu	16 (d)	1/2	1/2	1/2	3.13 (4)	1/2

Sb	16 (c)	0	0	0	1.35 (9)	1
O	48 (f)	0.3335 (2)	0.125	0.125	5.24 (9)	1
H3O+	8 (b)	0.375	0.375	0.375	1.97 (8)	0.36
O'	8 (b)	0.375	0.375	0.375	1.97 (8)	0.41
-	Rp=10.90	Rwp=11.4	$\chi^2=4.66$	RB=4.04	RF=4.15	a=0.2826 (8) Å

In these phases, antimony exhibit a low distorted octahedral environment in agreement with the values of the oxygen (O) positional parameter x (ideal theoretical value calculated for a regular octahedron: $x=0.3125$). The Sb-O distances are of the same order of magnitude in comparison with those raised in many oxide pyrochlores [20,21,29] and close to the theoretical value ($D_{\text{Shannon}}=0.62+1.40=2.02$ Å) [28].

TABLE 2. Interatomic distances (Å) and bond angles (°) for $(\text{H}_3\text{O}^+)_{0.36}\text{Ln}_x\text{Sb}_2\text{O}_6\text{O}'_y$.

$(\text{H}_3\text{O}^+)_{0.36}\text{Gd}_{0.80}\text{Sb}_2\text{O}_6\text{O}'_{0.38}$		$(\text{H}_3\text{O}^+)_{0.36}\text{Eu}_{0.82}\text{Sb}_2\text{O}_6\text{O}'_{0.41}$
$(\text{H}_3\text{O}^+)\dots\text{O}'$	3.038 (2) ($\times 2$)	2.996 (1) ($\times 6$)
Ln...O	2.525 (3) ($\times 6$)	2.225 (7) ($\times 2$)
Ln...O'	2.226 (3) ($\times 6$)	2.496 (2) ($\times 6$)
Sb...O	1.992 (3) ($\times 6$)	2.009 (1) ($\times 6$)
O'-Ln-O'	180.0	180.0
O-Ln-O	63.4 (1), 116.6 (1)	63.8 (4), 116.1 (6)
O-Ln-O'	79.2 (4)	78.5 (5)
O-Sb-O	83.5 (3), 96.4 (7)	83.0 (6), 97.9 (1)
Sb-O-Sb	131.6 (1)	129.4 (2)

Spectroscopy data infrared

The ions exchange reactions observed in the case the $\text{Na}_{0.36}\text{Ln}_x\text{Sb}_2\text{O}_{6+y}$ phase in acid medium and the reversibility of this phenomenon, could not constitute a formal proof of the existence of (H_3O^+) ions in the compound with expected formula $(\text{H}_3\text{O}^+)_{0.36}\text{Ln}_x\text{Sb}_2\text{O}_{6+y}$. In order to identify the accommodation of H_3O^+ ions in our compounds, the pyrochlore $(\text{H}_3\text{O}^+)_{0.36}\text{Ln}_x\text{Sb}_2\text{O}_{6+y}$ was studied by infrared spectroscopy. In spite of the data of the vibrational frequencies of H_3O^+ ion is obtained with systems chemically different from the samples studied in this work. They have given information about the presence H_3O^+ ion. We were inspired to benefit our spectra from work of Michel *et al.* for the compounds pyrochlores $\text{H}_2(\text{H}_2\text{O})\text{M}_2\text{O}_6$ with $\text{M}=\text{Nb}$, Y and HSbWO_6 , H_2O . The FT-IR transmission spectrum (FIG. 3) exhibits:

- Two bands located in the $450\text{-}750\text{ cm}^{-1}$ range, which characterize the antisymmetric vibration of valence of the connection antimony-oxygen Sb-O.
- The broad band in the $2900\text{-}3200\text{ cm}^{-1}$ range, it related the symmetrical and antisymmetric vibration modes of H_3O^+ ion.
- A diffuse band centered around 1750 cm^{-1} could be attributed to the antisymmetric deformation of H_3O^+ ion.
- A weak band centered around 1100 cm^{-1} which can be assigned to the symmetrical deformation of H_3O^+ ion.

These FT-IR data must be considered carefully because of the possible presence of water absorbed on the surface sample. A study by NMR spectra is then necessary to confirm the results obtained by FT-IR spectroscopy.

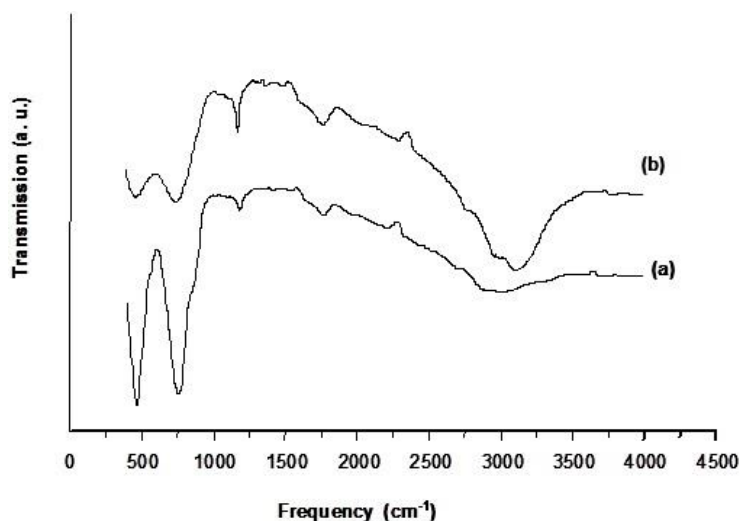


FIG. 3. (a) Infrared spectra for $(\text{H}_3\text{O}^+)_{0.36}\text{Gd}_{0.80}\text{Sb}_2\text{O}_{6.38}$ and (b) $(\text{H}_3\text{O}^+)_{0.36}\text{Eu}_{0.82}\text{Sb}_2\text{O}_{6.41}$.

Study of the $\text{Na}_{0.36}\text{Gd}_{0.80}\text{Sb}_2\text{O}_{6.38}$, $(\text{H}_3\text{O}^+)_{0.36}\text{Gd}_{0.80}\text{Sb}_2\text{O}_{6.38}$ and $(\text{H}_3\text{O}^+)_{0.36}\text{Eu}_{0.82}\text{Sb}_2\text{O}_{6.41}$ by ^{23}Na and ^1H solid state NMR

^{23}Na MAS NMR spectra of the $\text{Na}_{0.36}\text{Gd}_{0.80}\text{Sb}_2\text{O}_{6.38}$ starting material and the H_3O^+ exchanged samples are shown in FIG. 4. The spectrum of the as-synthesized $\text{Na}_{0.36}\text{Gd}_{0.80}\text{Sb}_2\text{O}_{6.38}$ compound exhibits a strong narrow band centred at 0.0 ppm. When this sample was washed several times with water, this narrow line decreased drastically in intensity, it is then related to impurities deposited on the powder surface during the synthesis. As a matter of fact, NaNO_3 was added in excess during the preparation of the samples. A consequent washing of these ones results in the decrease of its concentration.

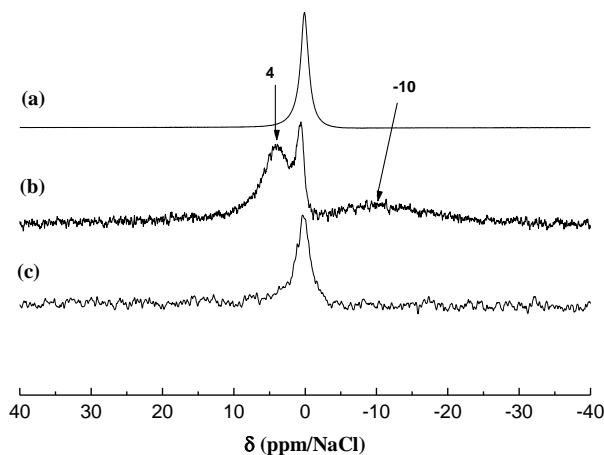


FIG. 4. (a) ^{23}Na MAS NMR spectra of the initial $\text{Na}_{0.36}\text{Gd}_{0.80}\text{Sb}_2\text{O}_{6.38}$ pyrochlore as-synthesized, (b) The sample washed several times with water, (c) The products resulting from the exchange of Na^+ by H_3O^+ .

After the washing, two broad bands are then observable at -10.0 and +4.0 ppm. The first one is consistent with hydrated sodium cations. Both the two broad lines could be attributed to the sodium ions located in the center of the hexagonal cavities of the pyrochlore framework. After exchange of Na^+ by H_3O^+ , these bands disappeared contrary to the narrow line of the impurity indicating the quasi-total exchange. The signal/noise ratio indicates a low content of residual ^{23}Na nuclei. A strong broad band between -25 and 40 ppm is present both in the static and ^1H MAS NMR spectrum of the $\text{Na}_{0.36}\text{Gd}_{0.80}\text{Sb}_2\text{O}_{6.38}$ sample (FIG. 5).

The absence of spinning bands for this line indicates that this contribution is not sensitive to the rotation of the sample. This peak is then certainly related to a disordered system with a distribution of chemical shifts which are not averaged by the MAS rotation. On the other hand, three fine lines, at 8.5 ppm, 8.3 ppm and 7.9 ppm (and their spinning side bands, which are well defined), are narrowed in the MAS conditions and are then related to two ^1H nuclei in ordered sites with one chemical shift tensor.

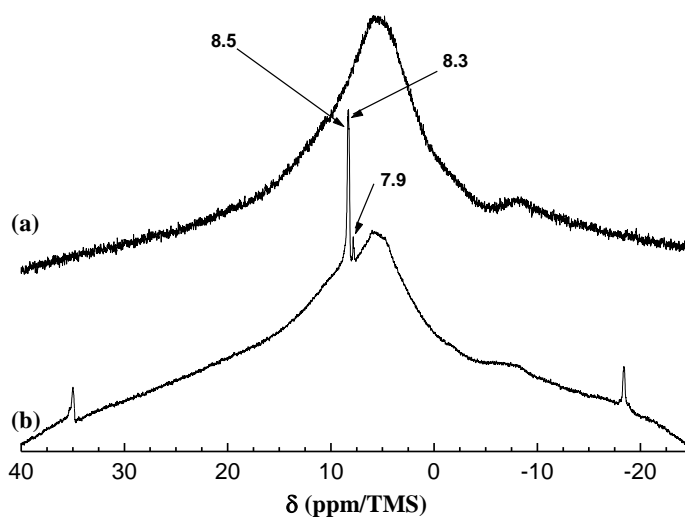


FIG. 5. (a) Static and (b) MAS ^1H NMR spectra of the initial $\text{Na}_{0.36}\text{Gd}_{0.80}\text{Sb}_2\text{O}_{6.38}$ pyrochlore.

The narrow lines are attributed to the water molecules located along the hexagonal tunnels of the host structure. An annealing treatment at 150°C for 2 hours in dynamic primary vacuum results in a low decrease of the relative intensity of the bands at 8.3 and 7.9 ppm in comparison with the one at 8.5 ppm (FIG. 6). On the contrary, after a thermal treatment at 700°C for 12 h in air atmosphere, all the narrow bands disappeared indicating that the water molecules are totally removed from the host inorganic matrix in these conditions. FIG. 7 shows the 300 MHz ^1H MAS NMR spectra of pyrochlore sample $\text{Na}_{0.36}\text{Gd}_{0.80}\text{Sb}_2\text{O}_{6.38}$ before and after ions exchange of Na^+ by H_3O^+ . The spectrum of the pyrochlore after exchanged by H_3O^+ is complex with at least 3 contributions at 10.8, 9.4 and 5.1 ppm.

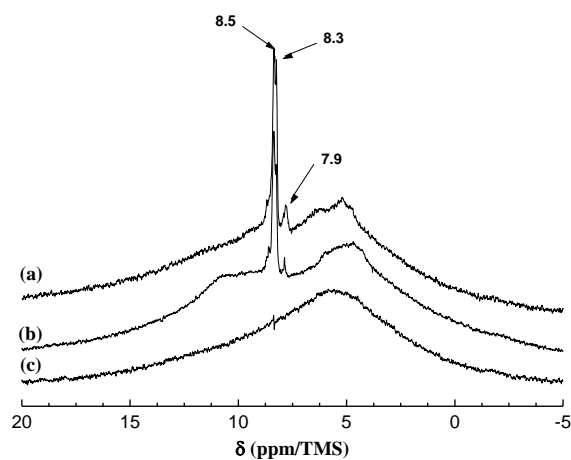


FIG. 6. (a) ^1H MAS NMR spectra of the $\text{Na}_{0.36}\text{Gd}_{0.80}\text{Sb}_2\text{O}_{6.38}$ pyrochlore as-synthesized and (b) after thermal treatments at 150°C in vacuum for 2 h and (c) at 700°C in air atmosphere for 12 h.

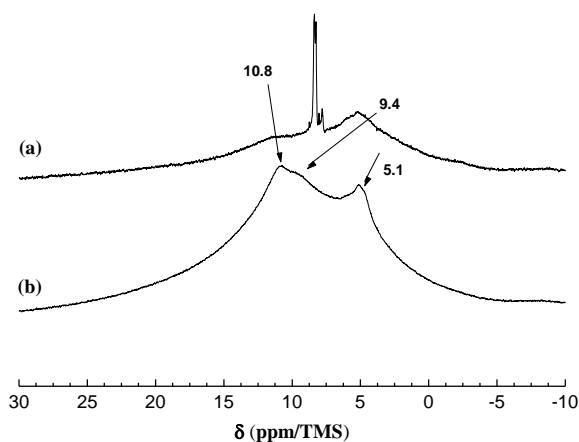


FIG. 7. (a) ^1H MAS NMR spectra of the $\text{Na}_{0.36}\text{Gd}_{0.80}\text{Sb}_2\text{O}_{6.38}$ pyrochlore, (b) The samples obtained after the exchange of Na^+ by H_3O^+ .

This suggests the existence of different H species in this latter sample; such a phenomenon was reported by Abraham et al. in the case of pyrochlore containing bismuth after exchange of potassium by proton. The presence of the band at 10.8 ppm indicates that the hydronium ions H_3O^+ are introduced into pyrochlore during the ions exchange processes; as a matter of fact, chemical shift value of these cations is expected at about 10 ppm. By comparison with NMR data concerning inorganic hydrated oxides, we can propose that the signal at 5.4 ppm is caused by protons of absorbed H_2O molecule.

^{13}Na and ^1H MAS NMR were also performed to characterize $\text{Na}_{0.36}\text{Eu}_{0.82}\text{Sb}_2\text{O}_{6.41}$ pyrochlore; this study reveals similar behaviours of these compound in comparison with $(\text{H}_3\text{O}^+)_{0.36}\text{Gd}_{0.80}\text{Sb}_2\text{O}_{6.38}$ pyrochlore during the exchange of sodium ions by H_3O^+ . This ^{13}Na and ^1H MAS NMR data show clearly the exchange of the sodium ions by H_3O^+ because of the disappearance of the bands of sodium ions and the presence of lines typical of the hydronium ions and H_2O after the exchange process.

Conclusion

Rietveld refinements of their X-ray powder patterns clearly show the formation of defect pyrochlore phases with a partial occupancy of the 16d sites by Gd^{3+} and Eu^{3+} ions and the 8 (b) site by H_3O^+ and O^{2-} ions. The ionic exchange properties in aqueous solution of pyrochlores containing sodium, rare earth and antimony ions were investigated for the first time. Such a process allows to form new pyrochlores where as a direct reaction of mixed appropriate oxides is unaffactive, thus could be synthesized. The structural refinements are in good agreement with the ^{23}Na and 1H solid state NMR and infrared spectroscopy characterization.

REFERENCES

1. Butler MA, Biefeld RM. Ionic motion in the defect pyrochlore NH_4TaWO_6 . *Sol Stat Comm.* 1979;29(1):5-7.
2. Binesh N, Bhat V, Bhat SV. Mechanism of protonic conduction in defect pyrochlore $HNbWO_6 \cdot xH_2O$ using MAS NMR. *Sol Stat Ion.* 1996;86:665-8.
3. Brunner DG, Tomandl G. A new proton-conducting ceramic: Part II. Preparation of proton-conducting $NH_{sub 4}NbWO_{sub 6}$ and $NH_{sub 4}TaWO_{sub 6}$. *Adv Ceram Mat.* 1987;2(4).
4. Goodenough JB, Hong HP, Kafalas JA. Fast Na^+ -ion transport in skeleton structures. *Mat Res Bull.* 1976;11(2):203-20.
5. Grins J, Nygren M, Wallin T. Studies on composition, structure and ionic conductivity of the pyrochlore type system $K_{1-x}Ta_{1-x}W_{1-x}O_6 \cdot nH_2O$, $0 < x < 1$. *Mat Res Bulletin.* 1980;15(1):53-61.
6. Isasi J, Lopez ML, Veiga ML, et al. Ionic conductivity of a new defect pyrochlore. *Sol Stat Ion.* 1996;89(3-4):321-6.
7. Michel C, Guyomarc'h A, Deschanvres A, et al. Nouveaux conducteurs ioniques caracterises par une structure a tunnels entrecroises. *Mat Res Bull.* 1978;13(3):197-203.
8. Duan N, Tian ZR, Willis WS, et al. Hydrothermal synthesis and structure of a potassium tantalum defect pyrochlore. *Inorg Chem.* 1998;37(18):4697-701.
9. Li YJ, Tsai PP. Lacunar pyrochlore-type tungsten oxides as humidity-sensing materials. *Sol Stat Ion.* 1996;86:1001-4.
10. Sato M, Abo J, Jin T. Structure examination of $NaLaNb_2O_7$ synthesized by soft chemistry. *Sol Stat Ion.* 1992;57(3-4):285-93.
11. Toda K, Honma T, Ye ZG, et al. Synthesis and structure determination of new layered perovskite compound, $KLnTa_2O_7$. *J Alloys and Comp.* 1997;249(1-2):256-9.
12. Gopalakrishnan J, Bhat V, Raveau B. $ALLnNb_2O_7$: A new series of layered perovskites exhibiting ion exchange and intercalation behavior. *Mat Res Bull.* 1987;22(3):413-7.
13. Baetsle LH, Huys D. Structure and ion-exchange characteristics of polyantimonic acid. *J Inorg and Nuclear Chem.* 1968;30(2):639-49.
14. Weigel F, Hoffmann G. The phosphates and arsenates of hexavalent actinides. Part I. Uranium. *J Less Common Met.* 1976;44:99-123.
15. Chowdhry U, Barkley JR, English AD, et al. New inorganic proton conductors. *Mat Res Bull.* 1982;17(7):917-33.
16. Perotoni CA, Haines J, Da Jornada JA. Crystal structure and phase transition in the defect pyrochlore NH_4NbWO_6 . *J Sol Stat Chem.* 1998;141(2):537-45.
17. El Haimouti A, Zambon D, M. EL-Ghozzi, D. Synthesis, structural and physico-chemical characterization of new defect pyrochlore-type antimonates $K_{0.42}Ln_{y'}Sb_2O_{6+z'}$ and $Na_{0.36}Ln_ySb_2O_{6+z}$ ($0 < y, y', z, z' < 1$; $Ln = Y, Eu$ and Gd) prepared by soft chemistry route. *J Alloys Comp.* 2004;363:130-4.

18. El Haimouti A, Zambon D, EL-Ghozzi M, et al. Synthesis and structural characterization of new defect pyrochlore type $A \times Ln_y Sb_2O_6^+ z$ antimonates ($0 < x, y, z < 1$; $A = Rb, Cs, Tl$; $Ln = Eu, Gd$ and Y) prepared by coprecipitation. *Mat Res Bull.* 2003;38:1423-36.
19. Fourquet JL, Jacoboni C, De Pape R. Les pyrochlores AIB_2X_6 : Mise en evidence de l'occupation par le cation AI de nouvelles positions cristallographiques dans le groupe d'espace $fd3m$. *Mat Res Bull.* 1973 Apr 1;8(4):393-403.
20. Darriet B, Rat M, Galy J, et al. Sur quelques nouveaux pyrochlores des systemes $MTO_3 WO_3$ et $MTO_3 TeO_3$ ($M = K, Rb, Cs, Tl$; $T = Nb, Ta$). *Mat Res Bulletin.* 1971;6(12):1305-15.
21. Rietveld H. A profile refinement method for nuclear and magnetic structures. *J App Crystall.* 1969 ;2(2):65-71.
22. Carvajal JR. Full prof: A program for the Rietveld Refinement and Pattern Matching Analysis", Abstracts of the satellite Meeting on Powder Diffraction of the XV Congress of the IUCr, Toulouse, France. 1991;pp:127.
23. Shannon RD. Revised effective ionic radii and systematic studies of interatomic distances in halides and chalcogenides. *Acta Crystallographica section A: Crystal Physics, Diffraction, Theoretical and General Crystallography.* 1976;32(5):751-67.
24. Piffard Y, Tournoux M. Structure du pyrochlore, $TlO, 51SbIII, 71SbV_2O_6, 32$. *Acta Crystallographica Section B: Struct Crystall and Crystal Chem.* 1979;35(6):1450-2.
25. Piffard Y, Dion M, Tournoux M. Structure cristalline du pyrochlore, $KO, 51SbIII, 67SbV_2O_6, 26$. *Acta Crystallographica Section B: Structural Crystallography and Crystal Chemistry.* 1978;34(2):366-8.
26. Michel C, Groult D, Raveau B. Ion exchange properties of pyrochlores AB_2O_6-I Preparation and structural study of new pyrochlores $AMWO_6 \cdot H_2O$ ($A = Li, Na, M = Nb, Ta, Sb$). *J Inorg Nuc Chem.* 1975;37(1):247-50.
27. Ciruolo MF, Hanson JC, Grey CP. Solid-state rubidium exchange of zeolite NH 4 Y. *Microporous and Mesoporous Materials.* 2001;49(1):111-24.
28. Feuerstein M, Hunger M, Engelhardt G, et al. Characterization of sodium cations in dehydrated zeolite NaX by ^{23}Na NMR spectroscopy. *Solid State Nuclear Magnetic Resonance.* 1996;7(2):95-103.
29. Zheng L, Fishbein KW, Griffin RG, et al. Two-dimensional solid-state proton NMR and proton exchange. *Journal of the American Chemical Society.* 1993;115(14):6254-61.